Nuclear Engineering and Design 253 (2012) 200–210

Contents lists available at SciVerse ScienceDirect

Nuclear Engineering and Design

journal homepage: www.elsevier.com/locate/nucengdes

Uncertainty and sensitivity analysis of the nuclear fuel thermal behavior

A. Bouloré[a,*], C. Struzik[a], F. Gaudier[b]

[a] Commissariat à l'Énergie Atomique (CEA), DEN, Fuel Research Department, 13108 Saint-Paul-lez-Durance, France
[b] Commissariat à l'Énergie Atomique (CEA), DEN, Systems and Structure Modeling Department, 91191 Gif-sur-Yvette, France

HIGHLIGHTS

- A complete quantitative method for uncertainty propagation and sensitivity analysis is applied.
- The thermal conductivity of UO_2 is modeled as a random variable.
- The first source of uncertainty is the linear heat rate.
- The second source of uncertainty is the thermal conductivity of the fuel.

ARTICLE INFO

Article history:
Received 5 April 2012
Received in revised form 22 August 2012
Accepted 23 August 2012

ABSTRACT

In the global framework of nuclear fuel behavior simulation, the response of the models describing the physical phenomena occurring during the irradiation in reactor is mainly conditioned by the confidence in the calculated temperature of the fuel.

Amongst all parameters influencing the temperature calculation in our fuel rod simulation code (METEOR V2), several sources of uncertainty have been identified as being the most sensitive: thermal conductivity of UO_2, radial distribution of power in the fuel pellet, local linear heat rate in the fuel rod, geometry of the pellet and thermal transfer in the gap. Expert judgment and inverse methods have been used to model the uncertainty of these parameters using theoretical distributions and correlation matrices.

Propagation of these uncertainties in the METEOR V2 code using the URANIE framework and a Monte-Carlo technique has been performed in different experimental irradiations of UO_2 fuel. At every time step of the simulated experiments, we get a temperature statistical distribution which results from the initial distributions of the uncertain parameters. We then can estimate confidence intervals of the calculated temperature. In order to quantify the sensitivity of the calculated temperature to each of the uncertain input parameters and data, we have also performed a sensitivity analysis using the Sobol' indices at first order.

© 2012 Elsevier B.V. All rights reserved.

1. Introduction

1.1. General context

Most of the physical phenomena occurring in nuclear fuel elements during their irradiation in nuclear power plants are controlled by the temperature. As a matter of interest, we can mention fission product release, fuel densification and swelling, creep of cladding and fuel, etc. In our fuel behavior simulation code, the models corresponding to all these phenomena are very much sensitive to the temperature calculated in the fuel. The confidence we have in the calculated behavior of the code depends mainly on the confidence in the calculated temperature.

1.2. Methodology

In the general framework of uncertainty analysis in fuel simulation codes, CEA follows the methodology recommended by the ESReDA organization (European Safety, Reliability and Data Association) (De Rocquigny et al., 2008). These recommendations consist of a decomposition of the global problem of uncertainties into four steps which have been adapted to our specific problem (Fig. 1).

First of all stands the specification of the problem (Step A). The fuel performance code we consider is the CEA code METEOR V2. It is a 1D-radial thermal–mechanical simulation code. The variable of interest is the central temperature in the fuel pellet which is calculated by a thermal model embedded in the METEOR V2 code (Struzik et al., 1997). The quantity of interest of this output variable

* Corresponding author. Tel.: +33 4 42 25 44 15; fax: +33 4 42 25 29 49.
E-mail address: antoine.boulore@cea.fr (A. Bouloré).

0029-5493/$ – see front matter © 2012 Elsevier B.V. All rights reserved.
http://dx.doi.org/10.1016/j.nucengdes.2012.08.017

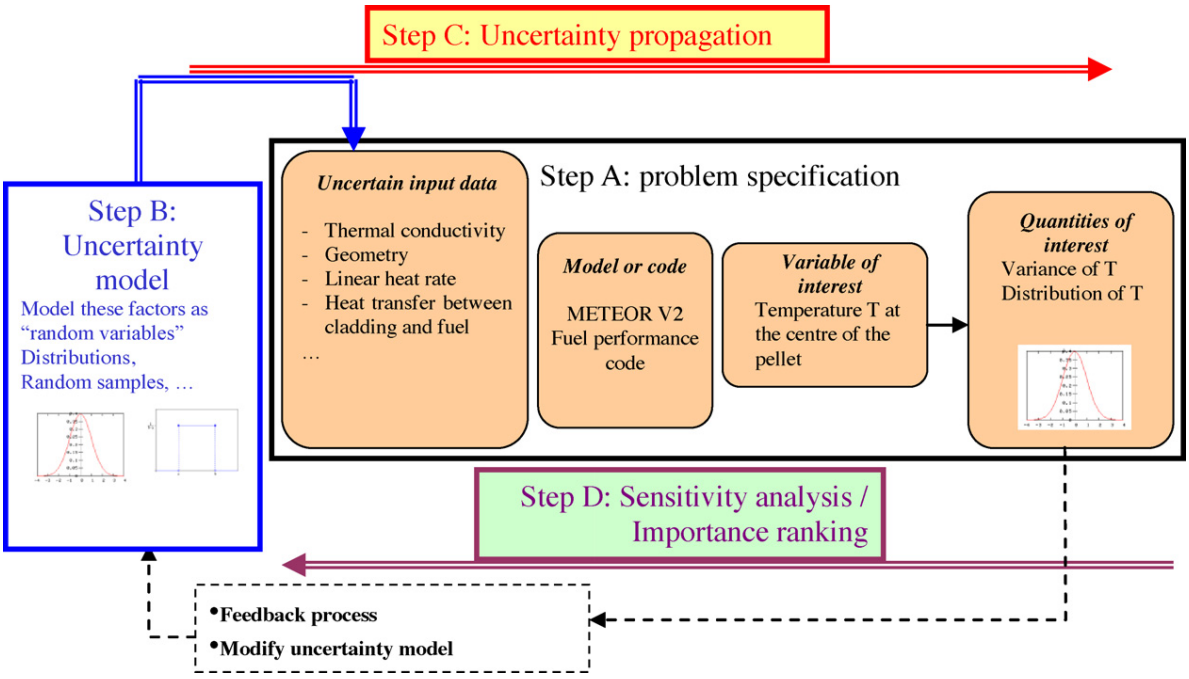

Fig. 1. General recommended methodology adapted to the thermal behavior simulation.

is mainly its variance, but also its whole distribution for different levels of temperature. Because the thermal model depends on the irradiation regime, in this paper we are interested in 2 different regimes:

- low burn-up, nominal PWR power;
- high burn-up, and transient regime.

To cover these 2 regimes, 2 experiments of interest are considered, and they are presented below (Section 1.3).

The calculation depends on a large number of input data such as geometry of the fuel elements, material thermal properties, filling gas composition in the free volume of the rod, irradiation power history, coolant temperature in the reactor, porosity of the pellet, corrosion behavior of the cladding, etc.

In the specification phase, the uncertain input parameters and data have to be listed. Depending on the considered experiment, we have limited the uncertain input parameters and data to:

- fuel thermal conductivity;
- linear heat rate;
- heat transfer between fuel pellet and cladding;
- divided into the transfer model itself, and the fuel pellet relocation model that controls the size of the gap;
- geometry of the pellet (inner radius in case of hollow pellet with a thermocouple);
- radial distribution of power.

The second step consists of the modeling of the uncertainties as random variables (Step B). The uncertainty model will be a set of parametric distributions (e.g. Uniform or Gaussian) with some independence hypotheses or approximate linear or rank correlations. This modeling has to be done as far as possible using all the experimental data available, and several methods can be used: direct observations, expert judgment, inverse methods, etc.

Once all the uncertain input parameters and data are modeled, the propagation through the code can be performed (Step C). This needs first the building of a design of experiment (DoE) of the input data (e.g. by a Monte-Carlo Sampling) which is propagated through the code to result in a representation of the variable of interest and a quantification of the quantities of interest mentioned above. Ideally, this step has to be completed by a sensitivity analysis step (Step D) which refers to the computation of sensitivity or importance indices of the uncertain input parameters with respect to the output variable. A large variety of methods are available, and in our case, we have focused on variance based methods (Sobol' indices). They quantify the part of the variance of the output variable due to the variance of each input parameters and data.

1.3. Experiments of interest

1.3.1. GRIMOX2

GRIMOX2 was an experiment conducted in the SILOE nuclear test reactor in Grenoble during the nineties (Caillot and Delette, 1998). It had been performed in order to study the thermal behavior of MOX fuel compared to the UO_2 fuel in the beginning of irradiation.

For that purpose a short fuel rod of PWR diametrical geometry including MOX and UO_2 pellets was irradiated in a boiling capsule pressurized to 13 MPa placed at the edge of the SILOE reactor core. At both ends of the experimental rod, the pellets were drilled in order to introduce a thermocouple. So this device allowed the measurement of the centerline temperature of both fresh fuel, UO_2 and MOX, during an irradiation up to 0.5 at%. The time duration of the experiment was about 4000 h (Fig. 2). The uncertainty on temperature measurement announced by the operator is $\pm 10\,^{\circ}C$.

The experimental fissile power was determined by the mean of neutron flux detector during the experiment and it was cross checked by quantitative gamma spectrometry after irradiation. The order of magnitude of power level is comparable to the PWR one in standard and incidental conditions.

Although two types of fuel had been tested in this experiment this paper only deals with the UO_2 stack.

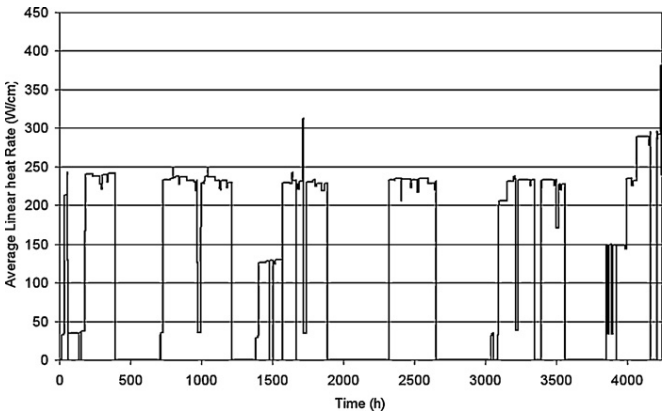

Fig. 2. Irradiation history of the GRIMOX2 experiment.

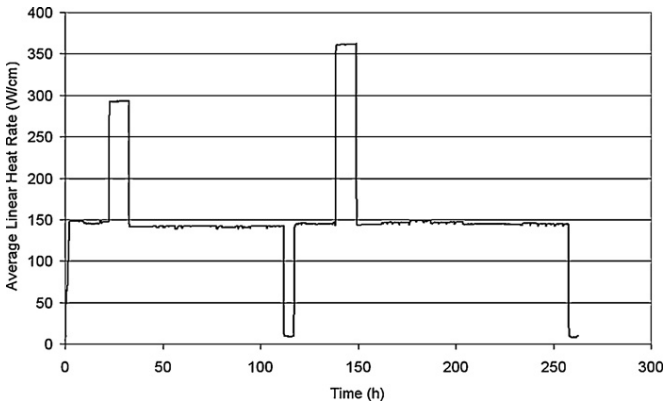

Fig. 3. Irradiation history of the REMORA2 experiment.

1.4. REMORA2

REMORA2 is an experimental irradiation conducted in the OSIRIS nuclear test reactor (Saclay). UO_2 chromium doped fuel, previously irradiated in a French PWR up to 62 GWd/tM, is re-irradiated at different levels of linear heat rate (Fig. 3), the aim of this type of experiment being to characterize the thermal behavior of the fuel at high burn-up (Muller et al., 2007). During the experiment, temperature at the center of the pellets at one end of the rod, and the inner pressure in the rod are measured.

1.5. The URANIE framework

The "Uncertainty and Sensitivity" platform URANIE developed by the CEA aims to capitalize all methods and algorithms about uncertainty and sensitivity in the same framework (Gaudier, 2010). URANIE is based on the data analysis framework ROOT (http://root.cern.ch), an object-oriented and petaflopic computing system developed by CERN. This framework offers several useful features as advanced visualization, powerful data storage and access in several formats (binary, SQL, distant access), a C++ interpreter, and so on.

URANIE is built in a modular way with several libraries (Fig. 4) devoted for a particular task in the Uncertainty and Sensitivity (US) analysis. We then describe the five libraries used in this study.

The main library defines the *TDataServer* object which contains the information about the uncertain variables for the US analysis. Then, this TDataServer object flows through the libraries in order to apply the methods of the study. For example, these methods fill or analyze the data.

The second library, the *Sampler* library, is devoted to generate a design of experiment (deterministic/statistical) from characteristics of the uncertain variables.

- qMC ("quasi Monte-Carlo") sequence (Sobol', Halton);
- SRS ("Simple Random Sampling"), LHS ("Latin Hypercube Sampling"), ROA ("Random Orthogonal Array"), Archimedean Copulas;
- MCMC ("Markov Chain Monte-Carlo") method for Gaussian mixture.

The *Launcher* library is devoted to manage the computation on a PC (sequential) or on a cluster (distributed). The goal is to construct the Y matrix (code/function results) jointed in the X

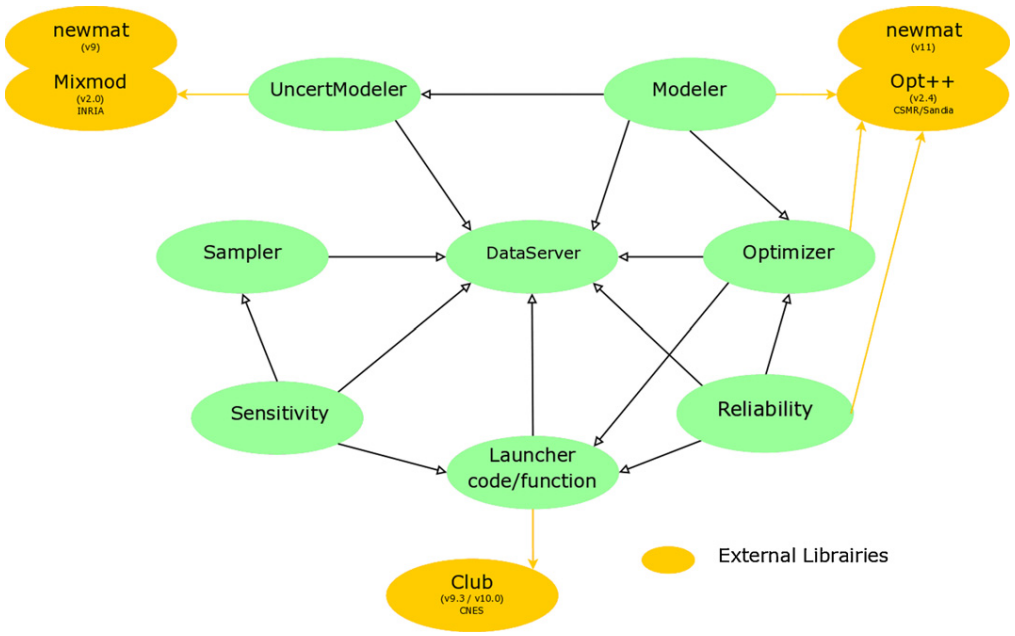

Fig. 4. Functional diagram of URANIE.

matrix (uncertain input parameters and data) of the design of experiment.

The *Sensitivity* library contains several methods for sensitivity analysis between the two *X* and *Y* matrix:

- Regression method (Pearson, Spearman);
- Screening method (Morris);
- Sobol' indices (Sobol', FAST).

The *Modeler* library is devoted to the building of "meta-models", i.e. analytical functions that can locally replace the original code with no computational cost (e.g. Artificial Neural Network, Linear regression, etc.).

ROOT, and so URANIE, have a C++ interpreter which allows us to integrate easily new algorithms or to customize complex treatment with several objects in a function with few parameters. The C++ interpreter is the first level of user interface. The second level user interface is an XML file; this file contains the description of the uncertain variables and the different steps to apply for US analysis.

2. Modeling of the uncertain input parameters

2.1. Thermal conductivity of UO_2 fuel

2.1.1. Unirradiated UO_2

Thermal conductivity of uranium dioxide changes with the irradiation history of the material. It is commonly admitted that its expression depends on temperature and burn-up (1),

$$\lambda(T,\tau) = \lambda_0(T) f_{deg}(T,\tau) \quad (1)$$

where λ_0 is the thermal conductivity of unirradiated fuel, and f_{deg} is a function describing its degradation due to irradiation history, represented by the burn-up τ (Lucuta et al., 1996).

In the following, we consider that the mathematical expression of the thermal conductivity of unirradiated uranium dioxide is a function of temperature T (in K) given by (2),

$$\lambda_0(T) = \frac{1-p}{1+cp}\left[\frac{1}{a+bT} + \frac{1}{T^{2.05}}\exp\left(d - \frac{e}{T}\right)\right] \quad (2)$$

where p is the porosity of the material, and the constants a, b, d, e are numerical parameters fitted on experimental measurements. Parameter c stands for the shape of the porosity in the material. Its value is contained between 0.5 and 2 (Olander, 1976; Marino, 1971).

Table 1
Description of the parameters of the thermal conductivity of unirradiated UO_2.

Parameter	Type of distribution	Parameters of the distribution	
a	Gaussian $N(m,\sigma)$	$m = 5.574 \times 10^{-2}$	$\sigma = 1.432 \times 10^{-2}$
b	Gaussian $N(m,\sigma)$	$m = 2.02 \times 10^{-4}$	$\sigma = 1.215 \times 10^{-5}$
c	Uniform U(min, max)	min = 0.5	max = 2
d	Gaussian $N(m,\sigma)$	$m = 23{,}847$	$\sigma = 0.9594$
e	Gaussian $N(m,\sigma)$	$m = 2.034 \times 10^4$	$\sigma = 2.714 \times 10^3$

Experimental values are available in a wide range of temperature, and for several batches of fuel which porosity changes from one batch to another. In addition to the scattering due to the different materials, each point results from a measurement, and the intrinsic experimental uncertainty (due to the experimental technique) on each of these points is ±20 K on temperature, ±7.5% on thermal conductivity below 2000 K, and ±20% above 2000 K. Having no more precise information on these uncertainties, we assume that they are described by uniform laws. To characterize the dispersion of these values, all of them have been normalized to 5% porosity (Fig. 5). On this graph, the line represents the law used in METEOR V2 and recommended by Lucuta et al. (1996).

Each experimental point being uncertain, the Monte-Carlo method is used to generate samples (random draw into the uncertainty intervals defined above for temperature and thermal conductivity using uniform distribution). So we get a large number of scatter charts, and for each, the parameters a, b, c, d and e from (2) are fitted using a least square minimization algorithm with constraints (especially for parameter c) available in the URANIE framework. Repeating this sampling-fitting sequence 5000 times leads us to get a sample of 5000 (a,b,c,d,e) vectors, so 5000 different expressions of the thermal conductivity λ_0.

Using this sample, it is possible to represent each scalar parameter by a theoretical distribution. First and second order of these distributions (expectation and variance), and correlation matrix of the vector, are the ones calculated from the sample (Table 1).

Coefficients of the correlation matrix (which is symmetric) are the linear correlation coefficients between 2 components x and y of the vector defined by (4):

$$\mathrm{corr}(x,y) = \frac{1}{n s_x s_y}\sum_{i=1}^{n}(x_i) - \bar{x}(y_i - \bar{y}) \quad (4)$$

n is the size of the sample, s_x and s_y are the standard deviations of the variables x and y calculated on the sample (Table 2).

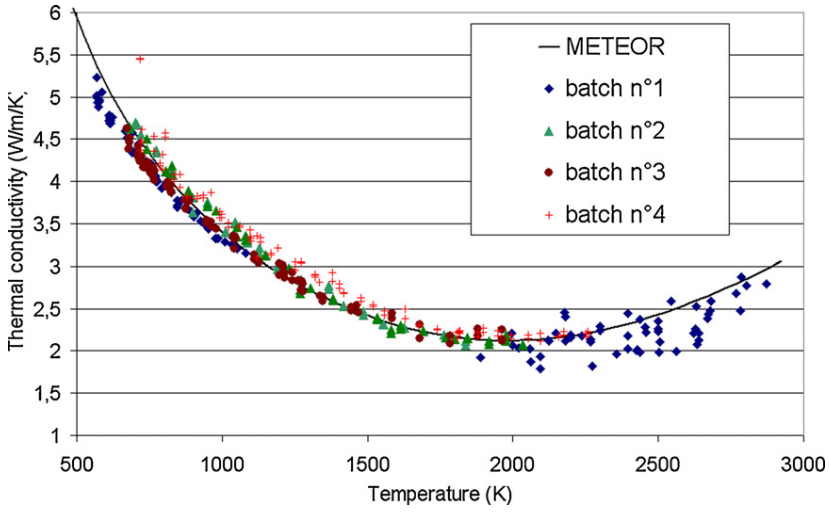

Fig. 5. Experimental values of thermal conductivity of UO_2.

Table 2
Pearson's correlation coefficients between the parameters of λ_0.

	a	b	c	d	e
a	1	−0.80	0.07	0.42	0.45
b		1	−0.30	−0.61	−0.64
c			1	0.10	0.07
d				1	1
e					1

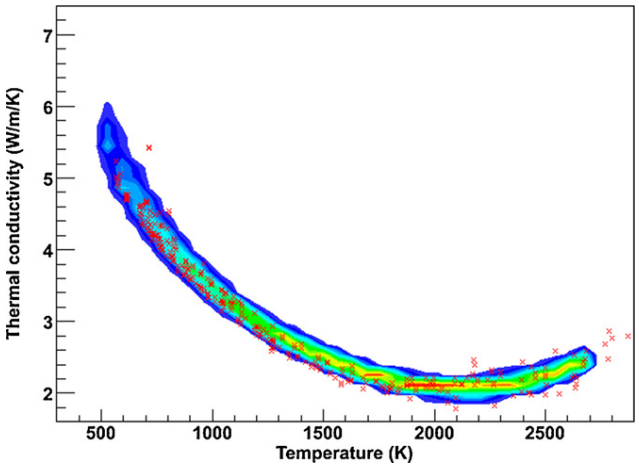

Fig. 6. Random variable λ_0 (contour plot) compared to experimental data (red points). (For interpretation of the references to color in this figure legend, the reader is referred to the web version of the article.)

Using these random parameters in the expression (2) leads to the definition of λ_0 as a complex random variable which covers the experimental scattering range, including its uncertainty (Fig. 6).

3. Irradiated fuel

The degradation of the thermal conductivity of irradiated UO_2 fuel we use is based on the recommendation by Lucuta et al. (1996). The degradation coefficient is a product of 3 factors, each representing a different phenomenon:

$$f_{deg}(T,\tau) = C_1(T,\tau)C_2(T,\tau)C_3(T,\tau) \quad (5)$$

where C_1 is the degradation due to dissolved fission products (FP), C_2 an improvement due to precipitated FP, and C_3 the effect of irradiation damage (irradiation defects).

Measurements on irradiated fuel samples have shown that the irradiation temperature has an effect on the accumulation of irradiation defects, and so impacts the thermal conductivity of the material. Moreover, when temperature changes, the material keeps transiently the memory of previous irradiation conditions. Then, when temperature increases, irradiation effects are annealed and their concentration reaches the equilibrium value corresponding to the new thermal state. The previous expression (5) does not reflect this effect despite the fact that it has been identified as a sensitive element by out of pile measurements.

As the matter of fact at each temperature, the adopted law describes an average state between a fully annealed state and damaged state which would correspond to the real irradiation temperature.

So for irradiated fuel, conductivity evaluation is generally slightly over predicted for base irradiation temperature under 1100 K or for the first steps of a high temperature transient regime following a base irradiation at low power, and slightly under predicted in the others cases.

But contrary to the fresh fuel case, there are too few experimental points available to define the uncertainty of each factor in (5). So only two uncertain factors are considered.

The first one is a global factor which allows the description of the fully damaged state; it is modeled by a normal distribution of mean 0.875 and of standard deviation 0.0141. This allows a correct description of the low power regime.

The second one allows the description of an instantaneous recovery temperature which has a direct effect on coefficient C_3. In the case where the irradiation temperature if higher than the temperature at which the conductivity is measured, the annealing of the defects is only partial and can be taken into account by using the following coefficient:

$$\mathrm{CF} = \frac{1}{2}\left(1 - \frac{T - T_{\mathrm{recovery}}}{200}\right)$$

which could be defined as a fraction of irradiation defects recovered at temperature T, T_{recovery} being the temperature at which all defects are recovered. This linear model is only a first approximation to try to take into account this recovery mechanism, and it does not include any kinetic aspect of the recovery. The irradiation defects effect on the thermal conductivity is modified from (Lucuta et al., 1996) to:

$$C_3(T,\tau) = 1 - 0.2CF\frac{1-\exp(-\tau)}{1+\exp((T-900)/80)}$$

The recovery temperature T_{recovery} is actually an unknown of the problem, which is modeled by a random variable following a uniform distribution between 950 and 1050 K.

It is noticeable that with this description, we are not able to describe the transient regime but the two fuel states damaged/annealed are described more correctly. Fig. 7 gathers fuel conductivity measurements at 55 GWd/tM collected in the literature (Ronchi et al., 2004; EPRI, 1999) and the proposed modeling. The values are normalized for 5% porosities.

A large scattering of the experimental data can be noticed. But the model proposed in this paper is in quite a good agreement with both series of data annealed or not.

The experimental values which are not covered by the modeling are relative to very low irradiation temperatures, characteristic of the external part of the pellet in PWR Reactor. So this part of fuel has no chance to reach a temperature between 1100 and 1400 K in standard irradiation conditions and would have to be considered only in accidental conditions (LOCA or RIA) when the temperature of outer part of the pellet could reach this level.

3.1. Thermal transfer between pellet and cladding

In the case of low burn-up experiments, the heat transfer between pellet and cladding depends on two different models: the model that controls the size of the gap, and the thermal transfer model itself. The uncertainty of these two models is considered separately.

3.1.1. Pellet fragments relocation model

In the METEOR code, this model calculates the radial repositioning of the fuel fragments due to the "diabolo" shape distortion of the pellet. In our code, the corresponding radial strain is supposed to be:

$$\varepsilon = \frac{u_{\mathrm{inter}} - u_{\mathrm{median}}}{2R} \quad (6)$$

where R is the outer radius of the pellet, u_{inter} and u_{median} are the radial displacements at mid-pellet and at inter-pellet planes given by numerical correlations functions of the linear heat rate and of the geometry of the pellets.

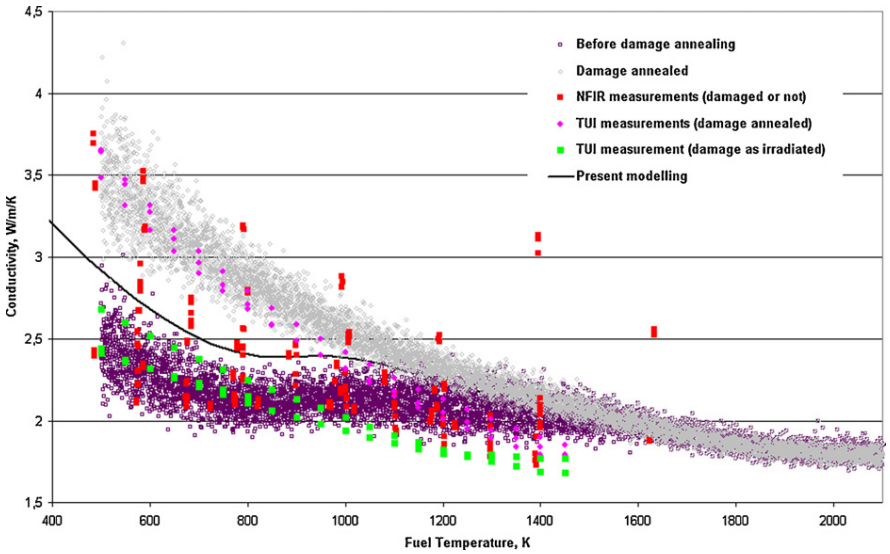

Fig. 7. Thermal conductivity compared to the experimental data at 55 GWd/t.

Two types of uncertainties have to be considered in this modeling. First, there is a global uncertainty on the numerical correlations, which can be modeled by a global factor (noted *bias_reloc* in the following) which represents the difference between a 3D simulation of the primary ridge and the measures performed after the irradiation. Following expert judgment, parameter *bias_reloc* is contained between 1 and 1.25, and has to be modeled in the following using a uniform distribution between these two values. Secondly, in (6) the factor 2 stands for the fact that the representative point in the 1D modeling is supposed to be the middle between the median plane and the inter-pellet plane. An uncertainty is reported on this factor, and using expert judgment, it is replaced by the *corr_inter_median_reloc* factor which distribution is supposed to be Gaussian (mean equal to 2 and standard deviation equal to 0.083).

4. Thermal transfer model

In the METEOR code, the thermal transfer between fuel and cladding is modeled using the URGAP model (Lassmann and Hohlefeld, 1987). The bulk heat transfer coefficient is the sum of 3 components: solid–solid contact (hcont), radiation (hr) and transfer through the gas (hg). Several numerical parameters appear in the expressions of these components. They have been determined either by best-estimate fitting, or by experimental measurement.

In the present paper, we only consider uncertainty on the numerical parameters introduced in the transfer through the gap (hg):

- β_3: model parameter of the gap conductivity,
- C_{Zr-He}: adaptation coefficient for the contact helium–zirconium,
- C_{UO_2-He}: adaptation coefficient for the contact UO_2–helium.

The modeling of β_3 as a random variable is arbitrary: we consider that the value of this parameter is contained between its best-estimate value $(1.369) \pm 50\%$, so it is defined by a uniform distribution between 0.68 and 2.00.

For parameters C_{Zr-He} and C_{UO_2-He}, experimental data exist. So C_{Zr-He} can be defined by a uniform distribution between 0.5 and 1.5, and C_{UO_2-He} by a uniform distribution between 0.21 and 0.33.

4.1. Radial distribution of power

In the METEOR V2 code, the radial distribution of power in the pellet is calculated using an improved version of the RADAR model (Palmer et al., 1992). A large number of uncertain numerical data are involved in this model (cross sections...). To model this uncertainty source, we use an inverse method. The reference code for neutron physics calculation of LWR at CEA is APOLLO2 (Santamarina et al., 2002) and its uncertainty is about 1% compared to a Kinetic Monte-Carlo neutronics code (TRIPOLI4) which is very accurate. So in this paper, we consider a tolerance on the calculated radial distribution of burn-up of 2% to be sure to cover the real uncertainty. We have identified 2 scalar parameters x_3 and x_4 in the RADAR model which allow controlling the radial distribution of power through the so-called 'Palmer's function':

$$f(r) = 1 + 3\exp[-x_3(r_{ext} - r)^{x_4}]$$

which describes the profile of plutonium production at a distance r of the center of the pellet, r_{ext} being the outer radius of the pellet. The inverse method principle is to define intervals of variation for x_3 and x_4 which leads to a radial distribution of burn-up in the uncertainty interval of the APOLLO2 simulation.

Min and max values are 7 and 15 for x_3 and 0.4 and 0.6 for x_4. Having no more information on an eventual probability density function (pdf), we assume uniform distributions in these intervals.

4.2. Linear heat rate

The determination of the uncertainty on the linear heat rate during an irradiation depends on the experiment itself, and it is difficult to generalize it to all experiments. So this paragraph is adapted to the experiments of interest developed later in this paper.

In the case of the GRIMOX2 irradiation, uncertainty on the linear heat rate has been estimated to 5%, but with no confidence interval relative to this value.

In the REMORA2 experiment, an evaluation of the uncertainty of the linear heat rate at the height of the thermocouple has been done from gamma scanning analysis. The enlarged uncertainty (equal to twice the standard deviation) has been estimated to 4.2%. Based on expert judgment, it appears that the relevant distribution to model

this random variable is the normal distribution. So, the linear heat rate in the experiment will be modeled by:

$$\mathrm{LHR} = \mathrm{LHR}_{\mathrm{measured}}(1 + \delta_{\mathrm{LHR}})$$

where $\mathrm{LHR}_{\mathrm{measured}}$ is the nominal experimental value, and δ_{LHR} is a random variable defined by a normal distribution of null expectation and standard deviation $\sigma = 0.021$.

Having no more precise information for the GRIMOX2 irradiation, the same model will be used for both experiments.

4.3. Geometry of the pellet (inner radius)

When propagation of the uncertainties is applied to experiments where the centerline temperature is measured, the geometry of the inner radius of the hole drilled in the pellets, where the thermocouple is inserted, has to be taken into account as an uncertainty source. The real radius of the hole does not correspond exactly to the specification, and as a matter of fact, the required modeling of this uncertain input depends on the experiment.

For the GRIMOX2 experiment, the specified inner diameter was equal to 1.3 mm. A few measurements performed after the drilling process show a scattering between 1.25 and 1.35 mm. Having no more precise information, the inner radius of the pellets where the thermocouple is inserted is considered as a random variable defined by a uniform distribution between 0.625 and 0.675 mm.

In the case of the REMORA2 irradiation, the same kind of measurements leads to the same modeling between 1.48 and 1.575 mm.

5. Propagation and sensitivity analysis

5.1. Principles

5.1.1. Uncertainty propagation

This is the phase which transforms the uncertainty of the input parameters and data to an uncertainty on the output (variable of interest) which is the centerline temperature in the fuel in our case. Most of the time, this phase consists of building a design of experiment of the uncertain input parameters and data using the models described in the previous section, and for each item of this sample, to perform a calculation of the variable of interest.

In this paper, we are interested in the scattering of the variable of interest, which we quantify by the variance of the centerline temperature, and so confidence intervals. Simulation method such as Monte-Carlo Sampling is well appropriate (De Rocquigny et al., 2008), and more precisely the Latin Hypercube Sampling, whose advantage is to be a 'stratified sampling without replacement' (Helton, 2006).

The centerline temperature being calculated at each time step of the simulation, for each set of the input parameters and data, a METEOR V2 calculation is performed that results in a calculated temperature history. The results are stored in a relational database and can be recalled and treated after the whole simulation. So the simulation process provides a distribution of calculated temperature histories, which can be represented by its first and second orders moments (mean m and variance σ^2).

6. Sensitivity analysis

Sensitivity analysis refers to the computation of sensitivity or importance indices of the uncertain input parameters with respect to the output variable. A large variety of methods are available in the literature (De Rocquigny et al., 2008). We have focused on the Sobol' indices method, which is variance-based (Sobol', 1993) and quantifies the part of the variance of the output variable due to the variance of each input parameter or data. Let $(X_i)_{1 \le i \le p}$ be the uncertain parameters, p the number of uncertain parameters, and T the temperature calculated by the METEOR V2 code. The total unconditional variance V of T can be decomposed as:

$$V(T) = \sum_{i=1}^{P} V_i + \sum_{i=1}^{P}\sum_{j>1} V_{ij} + \cdots + V_{12\ldots p}$$

where

$$V_i = V(E(T \,|X_i\,)),$$

$$V_{ij} = V(E(T \,|X_i, X_j\,)) - V_i - V_j$$

and so on.

Physically, V_i is a measure of the effect of the random variable X_i on T, V_{ij} measures the effect of the interaction between X_i and X_j on T, etc. To have a measure of the total effect of X_i on T, we have to add V_i and all the effects of interactions with the other uncertain inputs. Sobol' indices are defined as the ration between these conditional variances and the total unconditional variance of T:

$$S_i = \frac{V_i}{V(T)} = \frac{V(E(T \,|X_i\,))}{V(T)},$$

$$S_{ij} = \frac{V_{ij}}{V(T)}, \ldots$$

$S_{\mathrm{Ti}} = S_i + \sum_j S_{ij} + \cdots$ is the total sensitivity index of X_i, which includes all the eventual interactions of X_i with the other uncertain input data. By definition, sensitivity indices verify the relation:

$$\sum_i S_i + \sum_i \sum_{j>i} S_{ij} + \cdots + S_{12\ldots p} = 1$$

Quantification of the total indices needs a great amount of simulations, and in our case, first order indices give already a good idea of the sensitivity of the output to the corresponding input. The expression $1 - \sum_i S_i$ quantifies the effects of interactions. The sample generated in the propagation phase not being sufficient to calculate the first order indices, it is necessary to build a "meta-model" (or surrogate model) which will be used to generate additional samples without having to perform exact computations with the original code. This concept is used to significantly reduce the computation time. A surrogate model is a mathematical function which produces comparable results with respect to the output variable and quantities of interest, but which is much quicker or easier to compute. In the URANIE framework, the 'Artificial Neural Networks' (ANN) functionality is available and easy to use (Dreyfus et al., 2005).

The generation of the ANN the simulation database available is divided into 2 parts:

- "learning" base: about 80% of the database which is used to the "learning phase" of the ANN generation,
- "testing" base: 20% of the database is used to validate the ANN built in the previous phase, that means check that the surrogate model is predictive.

In this paper, we limit the size of the ANN to one hidden layer between the inputs and the scalar output. The learning of one connection of the ANN needs approximately 10 points of the database. So the number of nodes nH in the hidden layer can be set depending on the size N of the learning database and the number of scalar inputs of our problem nX:

$$N = 10 \times nN \times (nX + 2)$$

In this paper, and depending on the considered experiment, nX varies from 12 to 14, so if have about 1000 simulations, we can set $nH = 7$.

When the ANN has been built, it is used to generate several samples, each being used to evaluate the first order sensitivity indices using the exhaustive 'brute-force' method, i.e. a direct calculation of the conditional variance of the output.

This sensitivity analysis can be bone either for each scalar input, or by model by grouping the parameters (Saltelli, 2002). The repetition on several artificial samples gives an evaluation of the uncertainty of the sensitivity indices.

In this paper, we only calculate the sensitivity indices by model or group of parameters, because for each uncertain input parameter or data, the initial uncertainty depends on the lack of knowledge of the whole model.

For each model the first order sensitivity index is

$$S_i = \frac{V(E(T \mid M_i))}{V(T)}$$

where M_i stands for the group of parameters corresponding to the model i.

6.1. GRIMOX2 case

For this experiment, we consider the following uncertainty sources:

- thermal conductivity of UO_2 fresh fuel, its degradation not being relevant at such a low burn-up;
- linear heat rate;
- heat transfer through the gap;
- radial distribution of power;
- inner radius of the drilled pellets.

10000 simulations have been performed with the METEOR V2 code, which can be summarized on the Fig. 8. Detailed analysis is performed at some instants: 729 h, 1715 h, 3206 h and 4239 h. Detailed temperature histograms and quantile–quantile plots show that the calculated temperature can be modeled by a normal truncated distribution (Fig. 9), which means that the half-95% confidence interval is equal to 2σ. The standard deviation depends on the temperature level (Fig. 10).

During the irradiation, most of the experimental data are located in this confidence interval, and so, in the case of this experiment, the difference between the average simulation and measurements can be attributed to the lack of knowledge of the input parameters and data of the thermal behavior models of the code.

The sensitivity analysis is performed at different instants of the irradiation simulation. For this experiment, the size of the original design of experiment is large enough to enable the calculation of the first order sensitivity indices directly by the 'brute-force' method.

First order sensitivity indices show that at every time step of the experiment simulation, the model which introduces the most uncertainty is the thermal conductivity model, which explains about 40% of the total variability of the calculated temperature (Table 3). Then comes the uncertainty on the linear heat rate which explains between 25 and 35% of the variance of the result. The last line of the table indicates that interactions between the different models are negligible (Table 4).

6.2. REMORA2 case

For this experiment, we consider the following uncertainty sources:

- thermal conductivity of UO_2 fuel, including its degradation in irradiation;
- linear heat rate;
- radial distribution of power;
- inner radius of the drilled pellets.

1000 simulations have been performed with the METEOR V2 code, and they can be summarized on Fig. 11. At each time step of the simulations, the distribution of calculated temperatures follows a normal distribution, which means that the half 95% confidence interval is equal to 2σ. This standard deviation is about 50 K on the second high power plateau. During the irradiation, the experimental data are contained in this confidence interval, and so, as for the GRIMOX2 experiment, the difference between the average calculation and the experimental data can be attributed to the lack of knowledge of the input parameters of our code. As for the low burn-up experiment simulations, the standard deviation depends on the temperature level (Fig. 12). On this figure, only phase 1 is represented, because during phase 2, our code calculates a reopening of the gap due to fuel creep which has not been observed in the following PIE. Actually, we only model the mechanical contact between the fuel and the cladding, but not the strong chemical bonding due to the internal zirconia layer.

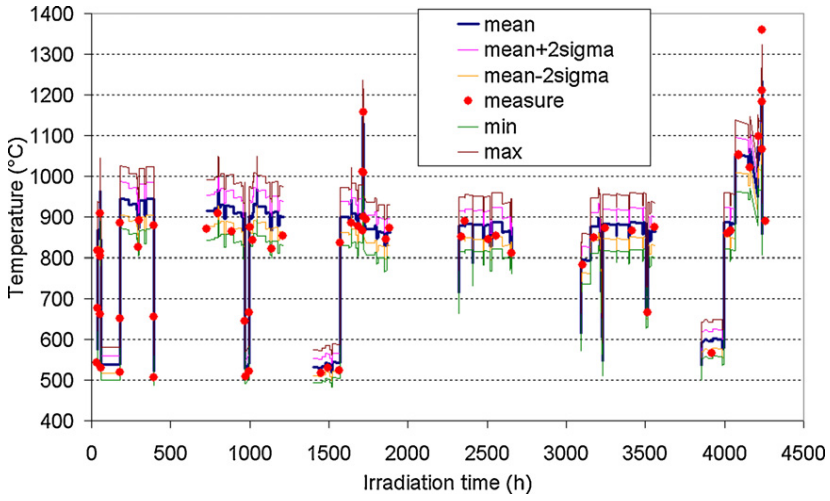

Fig. 8. Dispersion of the Monte-Carlo simulations (GRIMOX2).

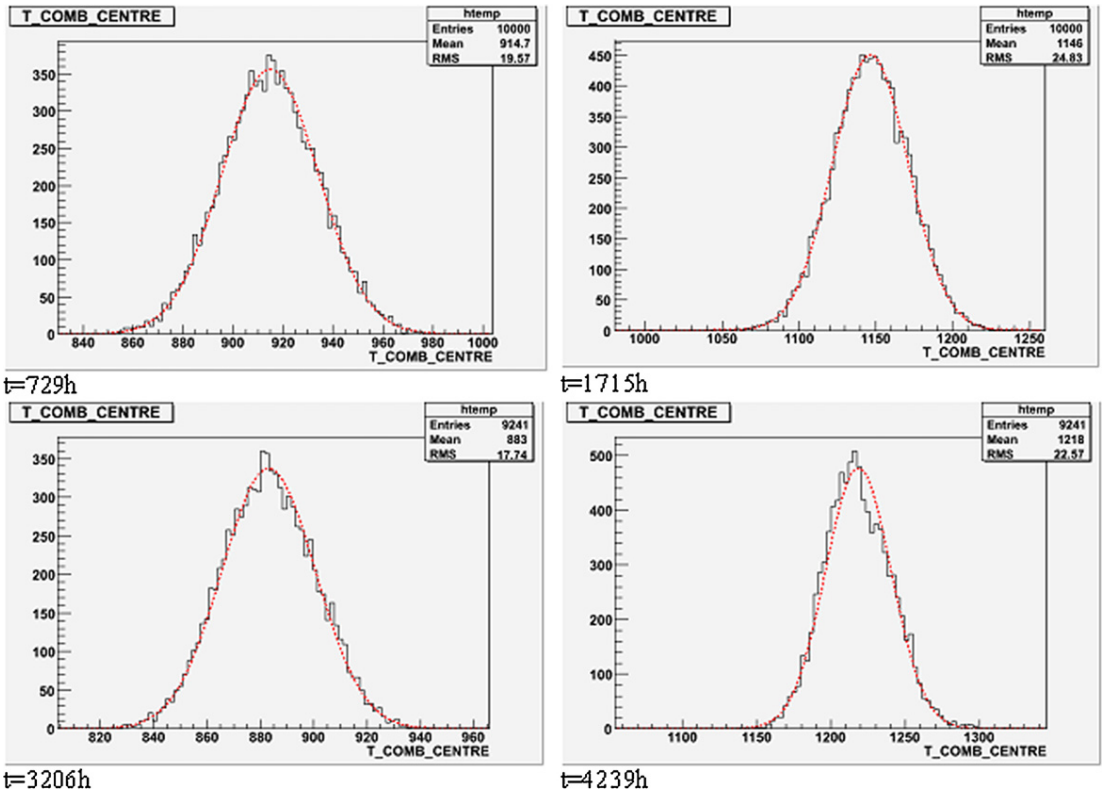

Fig. 9. Histograms of calculated temperature (GRIMOX2).

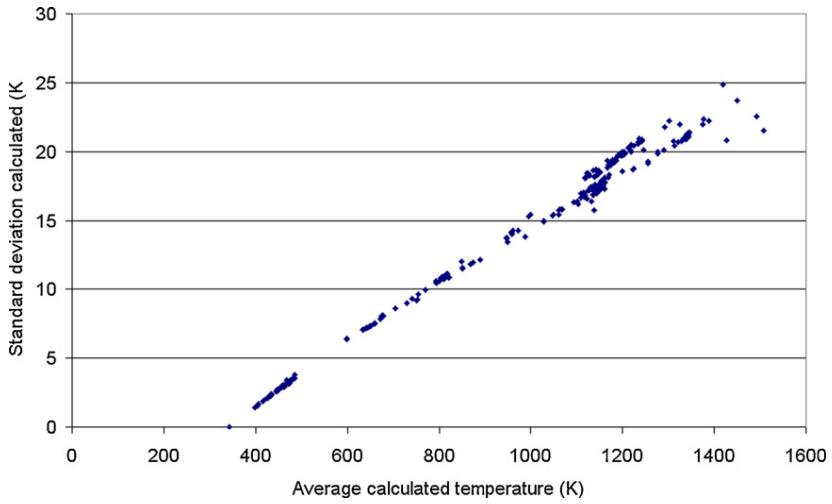

Fig. 10. Standard deviation of the calculated temperature (GRIMOX2).

Table 3
Sobol' indices for GRIMOX2 case.

Model	Sobol' first order indices			
	t = 729 h	t = 1715 h	t = 3206 h	t = 4239 h
Linear heat rate	0.33	0.34	0.26	0.26
Thermal conductivity of fresh fuel	0.42	0.38	0.42	0.41
Thermal transfer through the gap	0.17	0.17	0.15	0.14
Fuel fragments relocation	0.06	0.07	0.13	0.12
Radial distribution of power	0.00	0.01	0.02	0.03
Inner radius of fuel pellets	0.00	0.00	0.00	0.00
$\sum S_i$	0.98	0.97	0.98	0.96

Table 4
Sobol' first order indices by model (REMORA2).

Model	First high plateau (1)	Second conditioning plateau (2)	Second high plateau (3)
Thermal conductivity of fresh UO_2 fuel	0.47	0.60	0.48
Degradation of thermal conductivity due to irradiation	0.10	0.07	0.03
Linear heat rate	0.38	0.28	0.40
Radial distribution of power	0.02	0.01	0.08
Inner radius of fuel pellets	0.03	0.01	0.01
$\sum S_i$	1.00	0.97	1.00

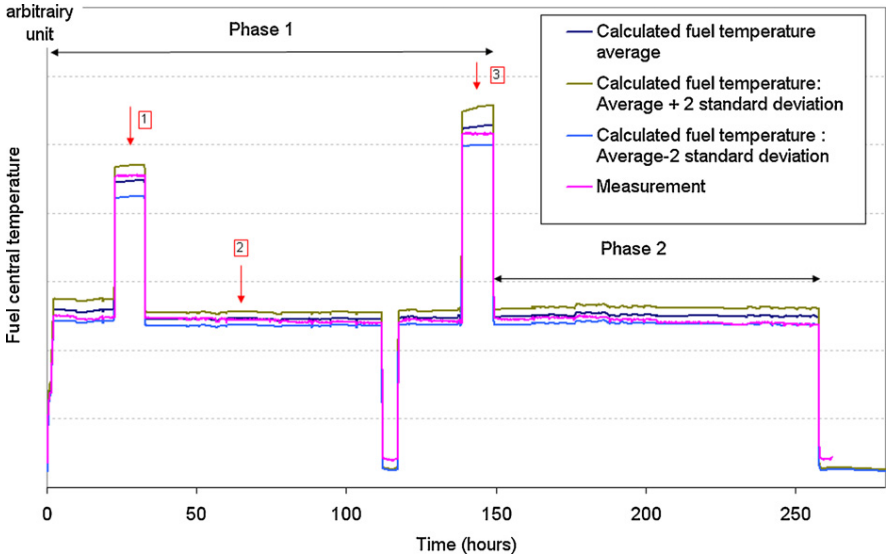

Fig. 11. Dispersion of the Monte-Carlo simulations (REMORA2).

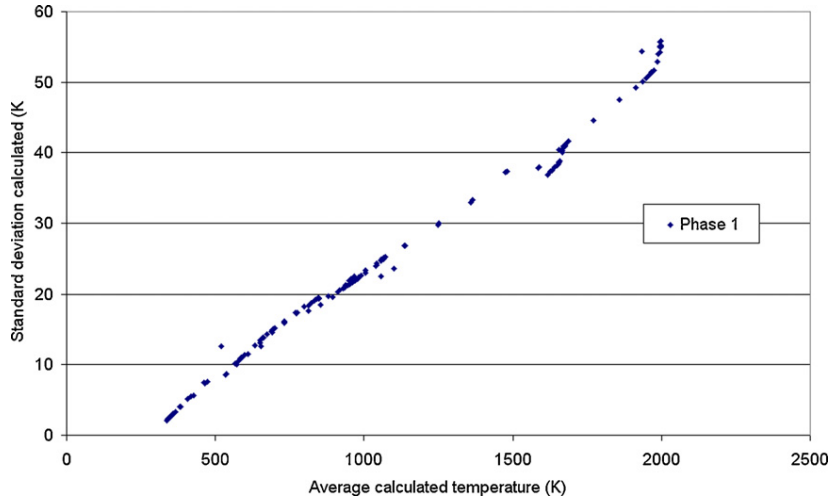

Fig. 12. Standard deviation of the calculated temperature (REMORA2).

Sensitivity analysis has also been performed at different instants of the simulation, noted 1, 2 and 3 on Fig. 11 on the same principle than for the GRIMOX2 experiment. But the original design of experiments contains only 1000 simulations, and is not large enough to apply the 'brute-force' algorithm. So at each of these instants, an ANN type surrogate model based on the original design of experiment is determined. This "meta model" is used to generate several samples containing about 10000 artificial simulations, and on each of them, the 'brute-force' algorithm is applied.

Sobol' first order sensitivity indices show that most of the variance of the calculated temperature is due to the uncertainty on thermal conductivity of unirradiated fuel (between 47 and 60%), and the linear heat rate of the experiment (between 28 and 40%). The effect of the uncertainty on the defects recovery effect on thermal conductivity is of third order (3–10%). The last line of the table indicates that interactions between the different models are negligible.

7. Conclusions

From a demonstrative point of view, the uncertainty process has been implemented in its totality: specification of the physical

problem, quantification and modeling of the uncertainty sources, uncertainty propagation and quantification of the variance of the calculated temperature, and last sensitivity analysis and importance ranking.

This process is validated by the fact that in the case of thermal irradiation experiments, the measurement is contained in the calculated confidence interval in both low and high burn-up tests.

In the case of low burn-up irradiation, the width of the 95% confidence interval of the calculated temperature is about ±15 K at 230 W/cm. For high burn-up and transient irradiations, this confidence interval is about ±80 K for a temperature around 1670 K and ±110 K around 1920 K.

In all cases, most of this uncertainty is due to the uncertainty on the linear heat rate, and to the lack of knowledge of the thermal conductivity of UO_2 either fresh or in irradiation condition.

This quantifies the reliability of our fuel performance code METEOR V2 in the area of thermal behavior simulation. Even if the uncertainty on calculated temperature seems limited, its impact on the calculation of other phenomena (fission gas release for example) can be more dramatic.

The uncertainty on the linear heat rate being irreducible because of the method used (Muller et al., 2007), the only way to improve the reliability of the calculated temperature is to reduce the uncertainty on the thermal conductivity of fresh UO_2 fuel. Improvements in the experimental technique (reduction of the uncertainty on each point) and more numerous data would help in this way.

References

Caillot, L., Delette, G., 1998. Phenomena affecting mechanical and thermal behaviour of PWR fuel rods at beginning of life: some recent experiment and modeling results. In: Proc. AEN-NEA Seminar on Thermal Performance of High Burn-up LWR Fuel, Cadarache, France (March 1998).

De Rocquigny, E., Devictor, N., Tarantola, S., 2008. Uncertainty in Industrial Practice: A Guide to Quantitative Uncertainty Management. Wiley, Chichester, West Sussex, UK.

Dreyfus, G., et al., 2005. Neural Networks – Methodology and Applications. Springer, New York.

EPRI, Palo Alto, Technical Report 111268, 1999. Understanding of thermal diffusivity recovery with thermal annealing.

Gaudier, F., 2010. URANIE: the CEA/DEN uncertainty and sensitivity platform. In: Procedia – Social and Behavioral Sciences, vol. 2, issue 6, Sixth International Conference on Sensitivity of Model Output, pp. 7660–7661.

Helton, J.C., et al., 2006. Survey of sampling-based methods for uncertainty and sensitivity analysis. Reliability Engineering and System Safety 91, 1175–1209.

Lassmann, K., Hohlefeld, F., 1987. The revised URGAP model to describe the gap conductance between fuel and cladding. Nuclear Engineering and Design 103, 215–221.

Lucuta, P.G., Matzke, H.j., Hastings, I.J., 1996. A pragmatic approach to modelling thermal conductivity of irradiated UO2: review and recommendations. Journal of Nuclear Materials 232, 166–180.

Marino, G.P., 1971. The porosity correction factor for the thermal conductivity of ceramic fuels. Journal of Nuclear Materials 38, 179–190.

Muller, E., Lambert, T., L'Hullier, N., Silberstein, K., Delafoy, C., Therache, B., 2007. Thermal behavior of advanced UO_2 fuel at high burnup. In: Proc. 2007 International LWR Fuel Performance Meeting, San Francisco.

Olander, D.R., 1976. Fundamental Aspects of Nuclear Reactor Fuel Elements, TID-26711-P1, National Technical Information Service. U.S. Department of Commerce, Springfield.

Palmer, I.M., Hesketh, K.W., Jackson, P.A., 1992. A model for predicting the radial power profile in a fuel pin. In: IAEA Specialists' Meeting on Water Reactor Fuel Element Performance Computer Modeling, Preston, March 1992.

Ronchi, C., Sheindlin, M., Staicu, D., Kinoshita, M., 2004. Effects of burn-up on the thermal conductivity of uranium dioxide up to 100,000 MWd/t. Journal of Nuclear Materials 327, 58–76.

Saltelli, A., 2002. Making best use of model evaluations to compute sensitivity indices. Computer Physics Communications 145, 280–297.

Santamarina, A., Chabert, C., Courcelle, A., Litaize, O., Willermoz, G., 2002. Qualification of the APOLLO2.5-CEA93 V6 for UOX and MOX fuelled PWRs. In: Proc. Int. Conf. PHYSOR 2002, Seoul, Korea, October 7–11.

Sobol', I., 1993. Sensitivity analysis for non-linear mathematical models. Mathematical Modelling and Computational Experiment 1, 407–414.

Struzik, C., Moyne, M., Piron, J.P., 1997. High burn-up modeling of UO_2 and MOX fuel with METEOR/TRANSURANUS version 1.5. In: Proc. Light Water reactor Fuel Performance Meeting, Portland, Oregon, March 1997.